Multifractal characterization of liquid water in clouds

Kristinka Ivanova*
Laboratoire de Télécommunications et Télédétection, Université Catholique de Louvain, Place du Levant 2, B-1348 Louvain-la-Neuve, Belgium

Thomas Ackerman
Department of Meteorology, Pennsylvania State University, 503 Walker Building, University Park, Pennsylvania 16802
(Received 11 May 1998; revised manuscript received 25 August 1998)

The variations of atmospheric quantities are often represented by highly fluctuating time series. Therefore, specially designed analysis tools are needed to study signals which vary on many scales. Recently, Davis *et al.* [J. Geophys. Res. **99**, 8055 (1994)] proposed a new technique for analysis of complex nonlinear geophysical processes observed over large time or space scales. The approach is aimed at investigating nonstationarity and intermittency as two complementary features of the geophysical fields. We apply the multifractal analysis to a liquid water path time series obtained via ground-based remote sensing measurements. On the (H_1, C_1) plane we compare the results from this study with the results of direct measurements of liquid water content during the same field program and those reported by other authors. [S1063-651X(99)11803-8]

PACS number(s): 02.50.−r, 05.40.−a, 05.45.Df, 05.45.Tp

I. INTRODUCTION

A new technique for data analysis of complex nonlinear geophysical processes observed over a large range of space and/or time scales has recently been proposed [1]. The technique is aimed at investigating nonstationarity and intermittency as two complementary features of geophysical data. These properties are especially pertinent to atmospheric data series due to the complex influence of external forces on and the internal variability of clouds. The approach seeks for various scales of self-affinity, i.e., searches for multiaffinity. It is a multifractal [2] data analysis tool developed specifically for turbulent cascade phenomenology [3,4] on one hand, and for characterization of nonlinear dynamical systems [5] on the other. The analysis involves first a criterion for stationarity of the data assuming a power-law behavior of the energy spectrum; the latter is ubiquitous in natural systems and phenomena [6]. Then two straightforward procedures are applied: singular measures and qth-order structure functions.

The singular measures approach seeks power-law behavior in integrals over all possible scales of a non-negative stationary field derived from the data, thus characterizing the intermittency. In contrast, the structure functions approach uses the data themselves to seek power-law dependence for the statistical moments of absolute increments over arbitrary large scales, thus leading to a quantitative and qualitative description of nonstationarity.

The multifractal approach was applied to study the statistical properties of liquid water content (LWC) spatial structure in marine stratocumulus clouds [1,7]. The authors analyze a large database of LWC time series collected by aircraft during the First ISCCP (International Satellite Cloud Climatology Project) Regional Experiment (FIRE) [8] and Atlantic Stratocumulus Transition Experiment (ASTEX) [9] field programs. Data collected in both experiments were obtained by direct measurements of the liquid water content when aircraft passed through cloud. We intend to apply the multifractal data series analysis to the remotely measured liquid water path (LWP) database obtained using a microwave radiometer and acquired by the Department of Meteorology of Pennsylvania State University during the ASTEX field program. The microwave radiometer measures the nadir emittance of the atmosphere at three microwave frequencies. These emittances are then used to retrieve total column water vapor and liquid water path. Liquid water path is the vertical integral of liquid water content. Because the structure of stratocumulus clouds is produced by ascending and descending air parcels and therefore vertically contiguous, we expect the variability in LWP to be similar to that of LWC. However, the field of view of the microwave radiometer is 5°, leading to a sample volume diameter of about 175 m at a height of 1 km. This larger sample volume smooths the LWP time series relative to the aircraft measured LWC time series.

Finally, it should be noted that this type of analysis turns out to be amenable to data of a very different nature from the above. Using the multiaffine fractal-like measures, Vandewalle and Ausloos [10] study the evolution of 23 foreign exchange currency rates (with respect to the Deutsche mark and Belgium franc, both for emerging markets and well controlled ones). These authors have shown that the behavior looks like a process of turbulence but with well- (3) separated ''categories'' depending on the involved money (strictly regulated european, hard dollar zone, emerging markets).

II. THE LWP DATA SETS AND THEIR SCALING PROPERTIES

We consider four data sets corresponding to four different days of observations, June 14, 15, 17, and 20, 1992 (Fig. 1).

*On leave from Institute of Electronics, Bulgarian Academy of Sciences, 72 Tzarigradsko chaussee, Sofia 1784, Bulgaria. Electronic address: kristy@ie.bas.bg

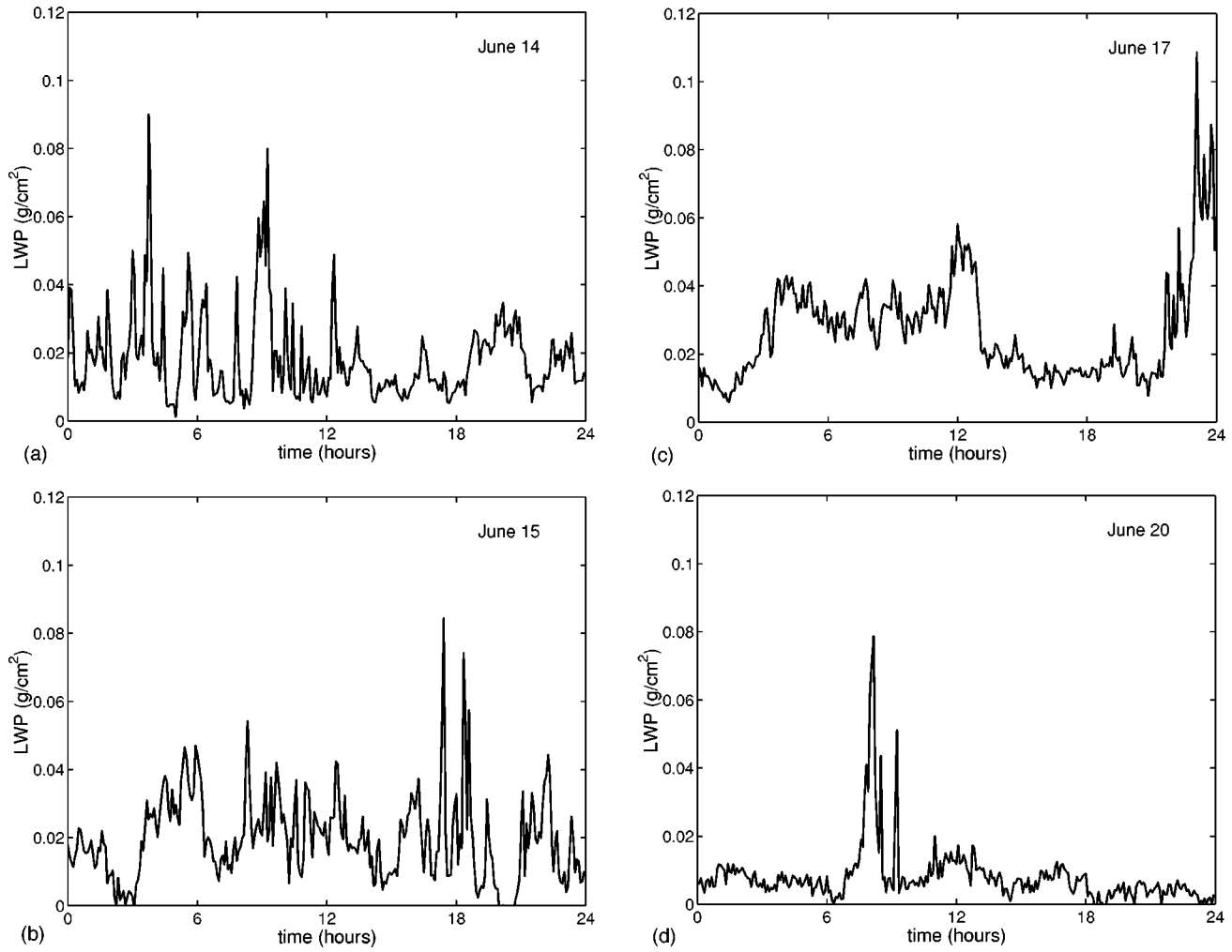

FIG. 1. The liquid water path (LWP) data sets measured with a microwave radiometer during the ASTEX'92 field program; the specific dates are (a) June 14, (b) June 15, (c) June 17, and (d) June 20.

They are chosen from among 26 data sets as being complete, that is, not containing missing observation points, and as forming a statistically homogeneous whole. Each profile is assumed to satisfy the Taylor's hypothesis [11]. The time resolution of the measurements is 5 min. Each data set contains 288 points covering a 24 h observation length.

If we knew the speed of the cloud displacement we could retrieve the discretization distance and then proceed with the analysis in space rather than in time. That would have given us a more direct comparison with FIRE and ASTEX in terms of distances, especially for the scaling ranges. It would, however, also assume that the cloud properties are invariant during the advection time. This assumption is certainly questionable, especially since our observations were taken on the windward side of an island.

The scale invariance properties of each of the data sets are first studied through their temporal power spectrum obtained from the Fourier transform of the data. Figure 2(a) depicts the spectrum $E(f)\sim f^{-\beta}$ averaged over the four data sets. The reference solid line corresponds to $\beta=1.49$. Due to the relatively short length of the series, their scaling range is not well defined. In an attempt to achieve better defined scaling limits, we analyze the second-order structure function which for a signal $\varphi(x_i), i=0,\ldots,\Lambda$, reads

$$D(r)=\langle|\varphi(x_{i+r})-\varphi(x_i)|^2\rangle \tag{1}$$

and scales as

$$D(r)\propto(r)^{\zeta(2)}. \tag{2}$$

The average is taken over all couples (x_{i+r},x_i). Figure 2(b) represents the best-line fit to the ensemble averaged $D(r)$ with $\zeta(2)=0.49\pm0.02$. The scaling range spans from the discretization time interval up to ≈ 1 h,35 min. The scaling range in the different sets is about the same. Only the June 17 data set exhibits a wider scaling range up to ≈ 2 h. The values of $\zeta(2)$ for the four data sets are included in Table I. Although it cannot be claimed that the scaling counterpart of the Wiener-Khinchin relation [12]

$$\beta=\zeta(2)+1 \tag{3}$$

holds for such short time series (hence not well-defined β), one can recognize the advantage in employing the $D(r)$ scaling properties in parallel with the spectrum analysis for estimating the spectral exponent. It should be noted also that the span of $\zeta(2)$ does not make a substantial difference when attributed to β. This is illustrated by the dashed lines in Fig. 2(a) (hardly recognizable). They correspond to spectral ex-

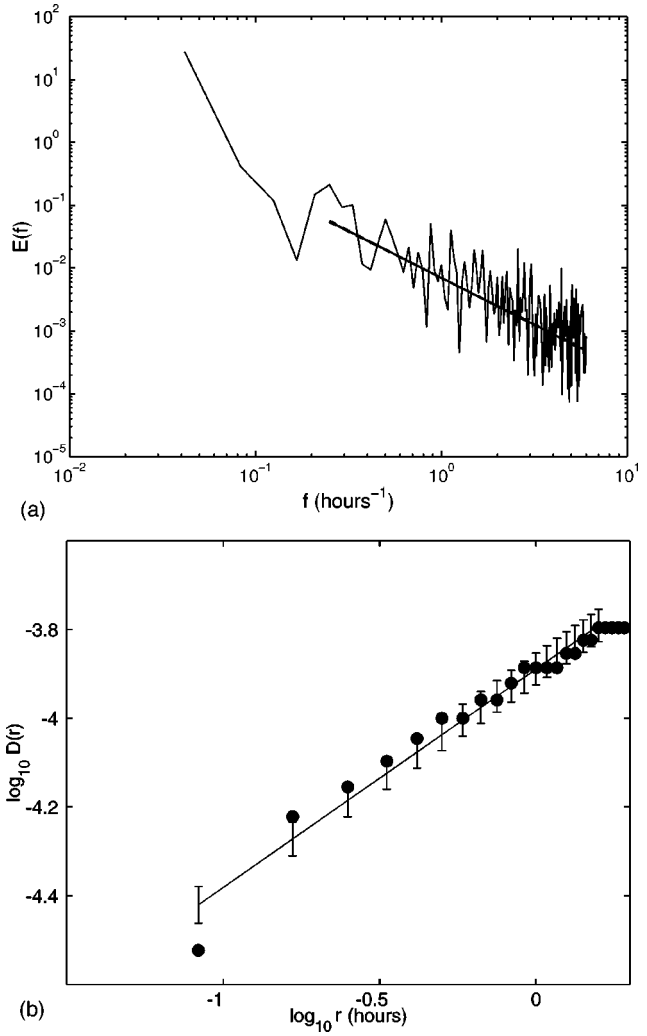

FIG. 2. Ensemble-averaged (a) power spectrum $E(f)$ and (b) second-order structure function for the remote sensing LWP data. The reference solid line corresponds to $\beta=1.49$. The dashed lines mark $\beta=1.49\pm0.12$. (b) The straight line represents the scaling fit with $\zeta=0.49\pm0.12$ up to about 1 h,35 min.

ponents $\beta=1.47\pm0.02$. The value of $\beta=1.49$ is somewhat greater than the spectral exponents reported by Davis *et al.* [1] for FIRE, $\beta=1.36\pm0.06$, and for ASTEX, $\beta=1.43\pm0.08$.

Arguments of stationarity are discussed at length by Davis *et al.* [1,13]. They can be summarized as follows. If $\beta<1$, then the process is stationary, that is, $\varphi(x)$ is statistically invariant by translation in x. If $\beta>1$, the signal is nonstationary. If in addition $\beta<3$, then the field has stationary increments, in particular, the small-scale gradient field will be stationary. Therefore, the data we analyze are nonstationary with stationary increments.

TABLE I. Summary of the nonstationarity (H_1) and intermittency (C_1) parameters for the four studied days and their ensemble average. The fourth column hosts values of $\zeta(2)$ and the last column hosts the values of $K(2)$.

Date	$\zeta(1)=H_1$	C_1	$\zeta(2)$	$K(2)$
June 14	0.24	0.09	0.45 ± 0.04	0.19
June 15	0.33	0.10	0.38 ± 0.02	0.20
June 17	0.28	0.08	0.67 ± 0.01	0.13
June 20	0.34	0.13	0.44 ± 0.02	0.27
Ensemble Averaged	0.29	0.10	0.49 ± 0.02	0.19

III. SINGULAR MEASURES AND qTH-ORDER STRUCTURE FUNCTIONS

The present section considers the intermittency and the nonstationarity features of the LWP data. The singular measure (SM) analysis of the small-scale gradient field obtained from the data is performed to account for the intermittency,

$$\varepsilon(r;l)=\frac{r^{-1}\sum_{i=l}^{l+r-1}|\varphi(x_{i+1})-\varphi(x_i)|}{\langle|\varphi(x_{i+1})-\varphi(x_i)|\rangle},\quad l=0,\ldots,\Lambda-r. \tag{4}$$

The scaling properties of the ensemble averaged qth order of the stationary field $\varepsilon(r;l)$ are sought,

$$\langle\varepsilon(r;l)^q\rangle\sim(r)^{-K(q)},\quad q\geqslant0. \tag{5}$$

A hierarchy of nondecreasing functions follows $C(q)=K(q)/(q-1)$ related also to the generalized dimensions $D(q)=1-C(q)$. Since $K(1)=0$, l'Hospital's rule in the limit of $q\to1$ provides a straightforward measure of inhomogeneity of the field,

$$C_1=\left.\frac{dK(q)}{dq}\right|_{q=1}, \tag{6}$$

where C_1 is an intermittency parameter [14]. The sparseness of the signal and presumably, therefore, of the quantity's distribution is characterized by C_1. Large C_1 describes a high level of intermittency and spikiness.

Multifractal analysis can also be conducted with the qth-order structure functions (SF),

$$\langle|\varphi(x_{i+r})-\varphi(x_i)|^q\rangle\sim t^{\zeta(q)},\quad q\geqslant0. \tag{7}$$

Among the nonincreasing exponents $H(q)=\zeta(q)/q$, the parameter of nonstationarity $H_1=H(1)$ has a geometrically meaningful interpretation [15,1], describing the roughness of the signal.

For each data set we apply the singular measures and structure functions analysis. First we calculate the singular measures and structure functions for values of q up to 3.8 for each day. Then an ensemble average is taken over the four data sets for every value of q. By applying a least-squares-fitting procedure to the structure functions in a log-log plot within the predefined range ($\leqslant1$ h,35 min), we estimate the exponent $\zeta(q)$. The same scheme is followed for the singular measures to assess the $K(q)$ function, but for the whole range of time intervals since this yields the lowest error-bar spread (Fig. 3). The value H_1 is highlighted by a circle, and a line tangent to $K(q)$ at $q=1$ is drawn to emphasize the $C_1=K'(1)$ estimate. For large q both functions suffer from the sampling limitations [1] as the structure function values become very small, making the analysis difficult

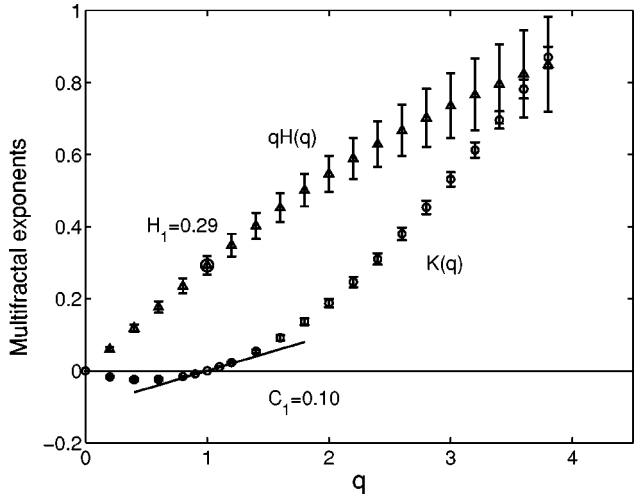

FIG. 3. Ensemble-averaged exponent functions $K(q)$ and $qH(q)=\zeta(q)$ as defined in the text by Eqs. (5) and (7) for the LWP data shown in Fig. 1.

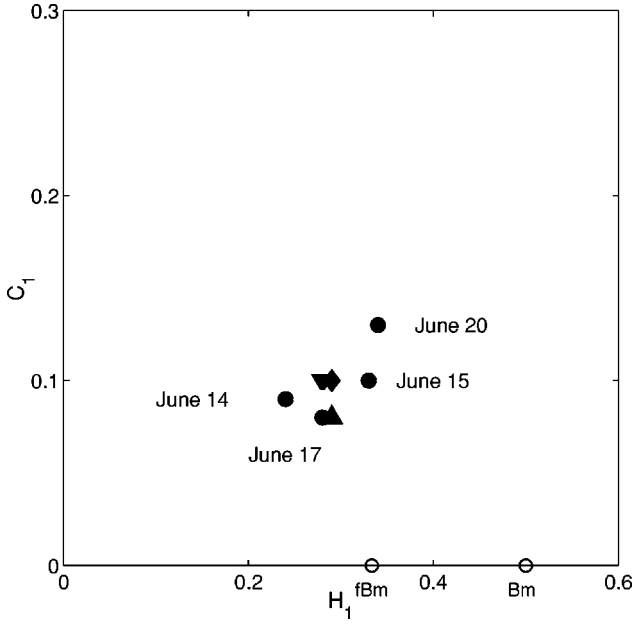

FIG. 4. The (H_1,C_1) plot summarizing the liquid water data results from the direct measurements during FIRE'87 (upside-down triangle) and ASTEX'92 (triangle) together with the remotely measured LWP during ASTEX marked by solid dots for individual days and by a diamond for their ensemble average. See Table I for (H_1,C_1) values for each day. The empty dots correspond to Brownian motion and fractional Brownian motion cases.

and resulting in larger error spreads for $\zeta(q)$. At the same time, $K(q)$ changes to a linear behavior which is interpreted to be the result of a single event dominating the statistics [1]. Such properties of the characteristic exponents were expected because of the relatively short data set. However, a nontrivial dependence for small and intermediate q is observed, namely, the concavity of the $\zeta(q)$ function which is interpreted to denote the multiaffinity [16] of the LWP field. The convexity of the $K(q)$ function reflects the multifractality of the absolute gradients of the field at small scales. Table I contains the specific values of the parameters of nonstationarity H_1 and intermittency C_1, as well as $K(2)$, for the four data sets studied and their averages. It should be noted that the standard multifractal inequalities $K(2)\geqslant C_1$ and $\zeta(2)/2\leqslant H_1$ are satisfied for all the cases except for June 17. For this data set the second inequality does not hold; this is attributed to a large burst of activity at the end in the corresponding Fig. 1(c), which imparts more statistical information to the prefactors in Eq. (7) than to the exponents.

In Fig. 4 the results for the two parameters are summarized on the (H_1,C_1) plane. The (H_1,C_1) dots corresponding to the four data sets are noted by solid dots. The diamond labeled ASTEX/RS marks the ensemble-averaged estimate corresponding to $H_1=0.29$ and $C_1=0.10$. On the same plane are drawn the results obtained by Davis *et al.* [1,13] and Marshak *et al.* [7] for directly measured LWC during the FIRE'87 (the upside-down triangle $H_1=0.28$, $C_1=0.10$) and ASTEX'92 (the triangle $H_1=0.29$, $C_1=0.08$) field programs. In addition, by empty dots are marked the Brownian motion (Bm) at $(H_1,C_1)=(0.5,\ 0)$ and the fractional Brownian motion (fBm) at $(H_1,C_1)=(1/3,\ 0)$. The latter emphasize the difference between the multifractal data and the standard monofractal model. We consider the close proximity of the nonstationarity and intermittency parameters for direct and remote measured liquid water as a strong indication of the reliability of the multifractal estimates obtained from the remote sensing measurements. Indeed, the intermittency parameter for all cases mentioned is within the range of $C_1=0.11\pm0.04$ for turbulent velocity fields, obtained by Marshak *et al.* [7] using the range of second-order exponents. This good agreement between *in situ* and remotely sensed statistical characteristics of boundary layer clouds suggests that long time series of ground-based observations can be used to deduce the structure of these clouds.

IV. CONCLUSIONS

We use multifractal singularity analysis and qth-order structure function analysis to study time series of LWP obtained via remote sensing measurements. The behavior of the ensemble-averaged characteristic exponents $\zeta(q)$ and $K(q)$ reflects the multifractal nature of the LWP record. The nonstationarity and intermittency of the real-world data are summarized in an (H_1,C_1) point (ASTEX/RS) in the ''mean multifractal plane.'' It is found to be very close to points obtained from directly measured LWC. The agreement confirms the usefulness of remote sensing for the characterization of the cloud structure in the lower atmosphere.

ACKNOWLEDGMENTS

K.I. gratefully thanks M. Ausloos for his comments on the manuscript. K.I. appreciates the hospitality of the Laboratoire de Télécommunications et Télédétection, Université Catholique de Louvain where she currently works under the SSTC Program of the Belgium government. Grant No. F-532 of the Bulgarian National Fund for Scientific Investigations is also acknowledged. T.A. acknowledges the support of the NASA FIRE Program for the collection of the ASTEX data and the support of the U.S. DOE, Atmospheric Radiation Measurement Program (Grant No. DOE DE-F602-90ER) for data analysis.

[1] A. Davis, A. Marshak, W. Wiscombe, and R. Cahalan, J. Geophys. Res. **99**, 8055 (1994); A. Davis, A. Marshak, W. J. Wiscombe, and R. F. Cahalan, in *Current Topics in Nonstationary Analysis*, edited by G. Trevilo, J. Hardin, B. Douglas, and E. Andreas (World Scientific, Singapore, 1996), pp. 97–158.

[2] G. Parisi and U. Frisch, in *Turbulence and Predictability in Geophysical Fluid Dynamics*, edited by M. Ghil, R. Benzi, and G. Parisi (North Holland, Amsterdam, 1985), pp. 84–88; T.C. Halsey, M.H. Jensen, L.P. Kadanoff, I. Procaccia, and B.I. Shraiman, Phys. Rev. A **33**, 1141 (1986).

[3] R. Benzi, G. Paladin, G. Parisi, and A. Vulpani, J. Phys. A **17**, 3521 (1984).

[4] J.L. McCauley, Phys. Rep. **189**, 225 (1990).

[5] A. Aharony, Physica A **168**, 479 (1990).

[6] B.B. Mandelbrot, *Fractals: Form, Chance, and Dimension* (W.H. Freeman, New York, 1977).

[7] A. Marshak, A. Davis, W. Wiscombe, and R. Cahalan, J. Atmos. Sci. **54**, 1423 (1997).

[8] B.A. Albrecht, D.A. Randall, and S. Nicholls, Bull. Am. Meteorol. Soc. **69**, 618 (1988).

[9] B.A. Albrecht, C.S. Bretherton, D. Johnson, W.H. Schubert, and A.S. Frisch, Bull. Am. Meteorol. Soc. **76**, 889 (1995).

[10] N. Vandewalle and M. Ausloos (private communication); Int. J. Mod. Phys. C **9**, 711 (1998).

[11] G.I. Taylor, Proc. R. Soc. London, Ser. A **164**, 476 (1938).

[12] A.S. Monin and A.M. Yaglom, *Statistical Fluid Mechanics* (MIT Press, Boston, 1975), Vol. 2.

[13] A. Davis, A. Marshak, W. Wiscombe, and R. Cahalan, J. Atmos. Sci. **53**, 1538 (1996).

[14] D. Schertzer and S. Lovejoy, J. Geophys. Res. **92**, 9693 (1987).

[15] J. Feder, *Fractals* (Plenum, New York, 1988).

[16] T. Viscek, and A.-L. Barabasi, J. Phys. A **24**, L845 (1991).